

Optimal Synthetic Aperture Method for Marine Controlled-Source EM Surveys

Daeung Yoon and Michael S. Zhdanov

Abstract—This letter introduces a novel approach to the optimal design of the synthetic aperture method for marine controlled-source electromagnetic (MCSEM) surveys. We demonstrate that the sensitivity of the MCSEM survey to a specific geological target could be enhanced by selecting the appropriate amplitude and phase coefficients of the corresponding synthetic aperture. We have developed a general optimization technique to find the optimal parameters of the synthetic aperture method. This approach makes it possible to increase the corresponding ratio between total and background fields within the area of an expected reservoir anomaly and, in this way, improve the resolution of the EM data with respect to potential subsurface targets. We also demonstrate that this optimal synthetic aperture method can be used for a removal of the distorting airwave effect from the MCSEM data collected in shallow water.

Index Terms—Electromagnetic, optimal, synthetic aperture.

I. INTRODUCTION

THE synthetic aperture method is based on designing sources with specific radiation patterns, which would “steer” a generated field in the direction of an area of interest [1]–[4]. A similar approach was recently discussed in [5], [6], where the authors applied a synthetic aperture method to the marine controlled-source electromagnetic (MCSEM) survey, formed by one line of transmitters and receivers. In [7], the authors applied a synthetic aperture method to MCSEM surveys with multiple lines of transmitters and receivers. The method uses the interference of the fields radiated by different sources to construct a virtual source with a specific radiation pattern, according to which the field is steered toward the target. In order to find the optimal parameters of the synthetic aperture that increases the EM anomaly, associated with the target, the authors of the cited papers searched for all the possible combinations of the parameters within the given ranges.

Another approach to achieving this goal is based on introducing data weights in order to increase the integrated sensitivity of a survey to a specific target area of subsurface formation. For example, it was demonstrated in [8] that data weighting could

dramatically affect the sensitivity distribution of a given survey. In [9] and [10], the authors demonstrated how the sensitivity of the MCSEM survey could be “controlled” by selecting the appropriate data weights. The controlled sensitivity also results in an increase in the anomalous EM response from the target.

The goal of this letter is to introduce a general optimization technique to find the optimal parameters of the synthetic aperture method. This approach makes it possible to increase the corresponding ratio between total and background fields within the area of expected target anomaly and, in this way, improve the resolution of the EM data with respect to potential subsurface targets. We also demonstrate that the optimal synthetic aperture method can be used for removal of a distorting airwave effect on MCSEM data collected in shallow water. As an illustration, we apply this method to the model exemplified by [7] and to analysis of the synthetic MCSEM data computer simulated for the Harding oil and gas field in the North Sea.

II. REPRESENTATION OF THE SYNTHETIC APERTURE METHOD USING DATA WEIGHTS

Consider a typical MCSEM geophysical survey, formed by a set of sea-bottom electric and magnetic field receivers, located at points with the coordinates \mathbf{r}_l , $l = 1, 2, \dots, L$. The transmitting horizontal electric bipole is towed behind the ship and sends a low-frequency EM field from points with coordinates $\tilde{\mathbf{r}}_j$, $j = 1, 2, \dots, J$. Receivers record the EM data, denoted by vector column $\mathbf{d}^{(l)} = [d_1^{(l)}, d_2^{(l)}, \dots, d_j^{(l)}]^T$, where the upper index l corresponds to the position of a receiver at point \mathbf{r}_j , and the component $d_j^{(l)}$ describes the response recorded by a receiver at point \mathbf{r}_l for a transmitter located at the point $\tilde{\mathbf{r}}_j$.

The synthetic aperture method is based on constructing a synthetic aperture source $G_A(\mathbf{r}; \omega)$ as a superposition of the spatially distributed sources $g(\mathbf{r}, \tilde{\mathbf{r}}_j \omega)$ located at the points $\tilde{\mathbf{r}}_j$, $j = 1, 2, \dots, J$, i.e.,

$$G_A(\mathbf{r}; \omega) = \sum_{j=1}^J a_j \exp(i\varphi_j) g(\mathbf{r}, \tilde{\mathbf{r}}_j \omega) \quad (1)$$

where a_j is an amplitude weighting, and φ_j is a phase shift [5]. We denote by $d_A^{(l)}$ the response recorded by receiver \mathbf{r}_l , $l = 1, 2, \dots, L$, for a synthetic aperture source G_A . Due to the superposition principle, this signal can be calculated as a linear combination of the responses for the original transmitters, i.e.,

$$\mathbf{d}_A = \mathbf{W}_A \mathbf{d} \quad (2)$$

where \mathbf{d} is a $[JL \times 1]$ vector column of the observed data,

$$\mathbf{d} = [\mathbf{d}^{(1)}, \mathbf{d}^{(2)}, \mathbf{d}^{(3)}, \dots, \mathbf{d}^{(L)}]^T \quad (3)$$

Manuscript received April 22, 2014; revised July 17, 2014; accepted July 25, 2014. This work was supported in part by the University of Utah Consortium for Electromagnetic Modeling and Inversion, by TechnoImaging, LLC, and by the Moscow Institute of Physics and Technology (MFTI).

D. Yoon is with the University of Utah, Salt Lake City, UT 84112 USA (e-mail: duyoon@gmail.com).

M. S. Zhdanov is with the University of Utah, Salt Lake City, UT 84112 USA, and TechnoImaging, LLC, Salt Lake City, UT 84107 USA. He is also with the Moscow Institute of Physics and Technology (MFTI), 140342 Zhukovskiy, Russia (e-mail: michael.s.zhdanov@gmail.com).

Color versions of one or more of the figures in this paper are available online at <http://ieeexplore.ieee.org>.

Digital Object Identifier 10.1109/LGRS.2014.2345416

\mathbf{d}_A is an $[L \times 1]$ vector column of the synthetic aperture data

$$\mathbf{d}_A = \left[d_A^{(1)}, d_A^{(2)}, d_A^{(3)}, \dots, d_A^{(L)} \right]^T \quad (4)$$

and \mathbf{W}_A is an $[L \times JL]$ block-diagonal rectangular matrix of the weights

$$\mathbf{W}_A = \begin{bmatrix} \mathbf{w}^{(1)} & 0 \dots & 0 \dots & 0 \dots \\ 0 \dots & \mathbf{w}^{(2)} & 0 \dots & 0 \dots \\ 0 \dots & 0 \dots & \ddots & 0 \dots \\ 0 \dots & 0 \dots & 0 \dots & \mathbf{w}^{(L)} \end{bmatrix}. \quad (5)$$

In the last formula, $\mathbf{w}^{(l)}$ is a $[1 \times J]$ vector row of the corresponding synthetic aperture weights w_j , i.e.,

$$\mathbf{w}^{(l)} = \left[w_1^{(l)}, w_2^{(l)}, \dots, w_J^{(l)} \right] \quad (6)$$

and

$$w_j^{(l)} = a_j^{(l)} \exp(i\varphi_j^{(l)}). \quad (7)$$

Application of the synthetic aperture weights, variable from receiver to receiver, is physically equivalent to “steering” the field generated from the transmitters in different directions for different receivers. As a result, one would obtain better “focusing” of the transmitting EM field on the geological target, e.g., the hydrocarbon (HC) reservoir.

III. DEFINITION OF THE OPTIMAL SYNTHETIC APERTURE FOR THE MCSEM SURVEY

For simplicity, we consider now the case of the weights, independent of the receiver positions. We also assume that the recorded data represent the inline component of electric field. In this case, (2) can be simplified as follows:

$$\mathbf{d}_A = \begin{bmatrix} E_1^{(1)} & E_2^{(1)} & \dots & E_J^{(1)} \\ E_1^{(2)} & E_2^{(2)} & \dots & E_J^{(2)} \\ \vdots & \vdots & \ddots & \vdots \\ E_1^{(L)} & E_2^{(L)} & \dots & E_J^{(L)} \end{bmatrix} \begin{bmatrix} w_1 \\ w_2 \\ \vdots \\ w_J \end{bmatrix} = \mathbf{E}\mathbf{w} \quad (8)$$

where \mathbf{E} is an $[L \times J]$ matrix of rearranged observed inline components of electric fields $E_j^{(l)}$ recorded by a receiver at point \mathbf{r}_l for a transmitter $\tilde{\mathbf{r}}_j$, and \mathbf{w} is a $[J \times 1]$ vector column of the corresponding synthetic aperture weights w_j , i.e.,

$$\mathbf{w} = [w_1, w_2, \dots, w_J]^T, \quad w_j = a_j \exp(i\varphi_j).$$

By analogy with (4), we denote by $d_B^{(l)}$ the electric field response recorded by receiver \mathbf{r}_l , $l = 1, 2, \dots, L$, for a synthetic aperture source computed for a geoelectrical model with the known background conductivity. Similar to (8), the synthetic aperture response for the background geoelectrical model \mathbf{d}_B can be expressed as follows:

$$\mathbf{d}_B = \mathbf{E}^b \mathbf{w} \quad (9)$$

where \mathbf{E}^b is an $[L \times J]$ matrix of rearranged background electric fields, and \mathbf{d}_B is an $[L \times 1]$ vector column

$$\mathbf{d}_B = \left[d_B^{(1)}, d_B^{(2)}, d_B^{(3)}, \dots, d_B^{(L)} \right]^T.$$

The vector column \mathbf{d}_R of the ratio between the observed inline electric fields and the background fields of the synthetic aperture can be expressed as follows:

$$\mathbf{d}_R = \left[\frac{d_A^{(1)}}{d_B^{(1)}}, \frac{d_A^{(2)}}{d_B^{(2)}}, \dots, \frac{d_A^{(L)}}{d_B^{(L)}} \right]^T = \mathbf{A}(\mathbf{w}) \quad (10)$$

where

$$\frac{d_A^{(l)}}{d_B^{(l)}} = \frac{\left[\sum_{j=1}^J E_j^{(l)} w_j \right]}{\left[\sum_{j=1}^J E_j^{b(l)} w_j \right]}$$

and \mathbf{A} is a forward operator for the normalized synthetic aperture data \mathbf{d}_R , which is a function of the synthetic aperture weights \mathbf{w} . The fundamental concept of the synthetic aperture method is based on an assumption that one can design a synthetic aperture source that will steer the EM energy toward the target and, in this way, increase the ability to detect the target by increasing the anomalous response from the target [5], [6]. This effect can be automatically achieved by selecting the synthetic aperture weights with the property that they magnify the normalized synthetic aperture data \mathbf{d}_R in the anticipated area of the location of the potential target. For example, let us introduce a vector column \mathbf{P} describing a designed normalized synthetic aperture data, which have a maximum over a specific area of the survey where we would like to steer the EM energy from a synthetic aperture source. We will determine the optimal synthetic aperture weights by solving a minimization problem for the following objective functional:

$$P(\mathbf{w}) = \|\mathbf{P} - \mathbf{A}(\mathbf{w})\|^2 + \alpha \|\mathbf{w}_n - \mathbf{w}_{\text{apr}}\|^2 = \min \quad (11)$$

where α is a regularization parameter

We can solve the minimization problem (11) by using the regularized conjugate gradient method as follows [11]:

$$\begin{aligned} \mathbf{r}_n &= \mathbf{A}(\mathbf{w}_n) - \mathbf{P}, \\ \mathbf{l}_n &= \mathbf{F}_n^T \mathbf{r}_n + \alpha(\mathbf{w}_n - \mathbf{w}_{\text{apr}}), \\ \beta_n &= \frac{\|\mathbf{l}_n\|^2}{\|\mathbf{l}_{n-1}\|^2}, \quad \tilde{\mathbf{l}}_n = \mathbf{l}_n + \beta_n \tilde{\mathbf{l}}_{n-1}, \quad \tilde{\mathbf{l}}_0 = \mathbf{l}_0, \\ k_n &= \frac{(\tilde{\mathbf{l}}_n^T \mathbf{l}_n)}{\left(\|\mathbf{F}_n \tilde{\mathbf{l}}_n\|^2 + \alpha \|\tilde{\mathbf{l}}_n\|^2 \right)}, \\ \mathbf{w}_{n+1} &= \mathbf{w}_n - k_n \tilde{\mathbf{l}}_n \end{aligned}$$

where \mathbf{F} is the Fréchet derivative matrix of the operator \mathbf{A} at iteration n , which can be analytically found by calculating the first variation of \mathbf{A} , and \mathbf{w}_{apr} is some *a priori* estimate of the data weights. We usually select the *a priori* data weights as units, which correspond to the case of uniform synthetic aperture. This ensures a stable solution of the inverse problem.

Once we find the synthetic aperture weights $\mathbf{w} = [w_1, w_2, \dots, w_J]^T$, we can convert them into the synthetic aperture parameters as follows:

$$a_j = |w_j| \quad \varphi_j^{(l)} = \arg(w_j).$$

This concludes the definition of the optimal synthetic aperture for the MCSEM survey.

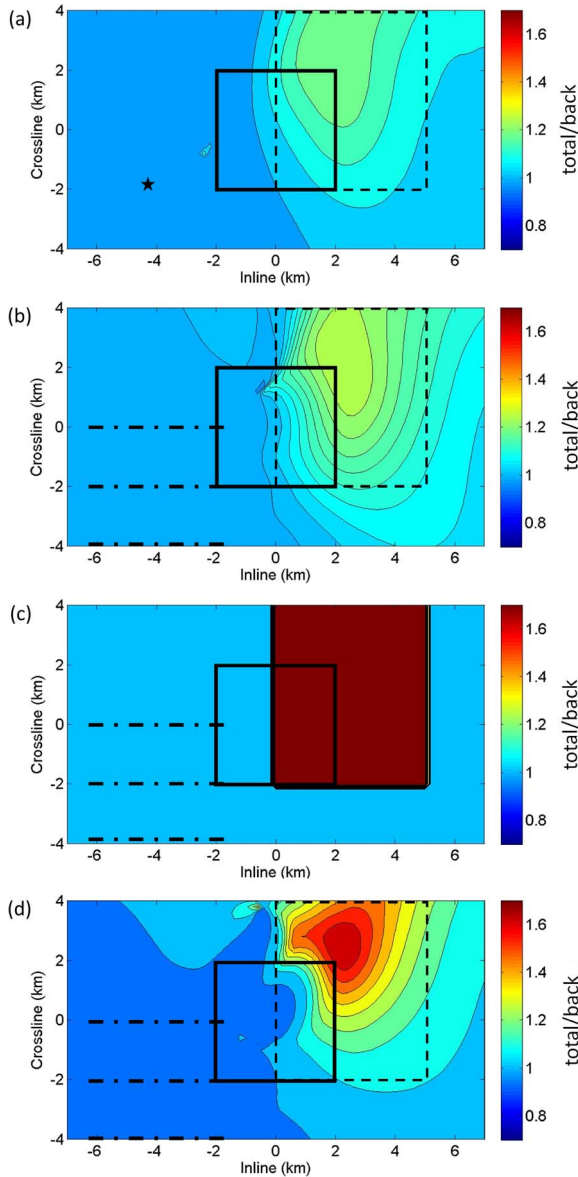


Fig. 1. Deep water model. (a) Original plot of the normalized data by a single source. (b) Normalized synthetic aperture data without steering. (c) Plot of the designed normalized synthetic aperture in a form of boxcar function covering the area of the expected reservoir anomaly. (d) Similar data produced by our optimal synthetic aperture method.

IV. NUMERICAL MODEL STUDY

Knaak *et al.* [7] presented an example of the application of synthetic aperture method to a 3-D synthetic CSEM data with a 2-D source distribution. We used the same model to demonstrate the advantages of the developed optimal synthetic aperture method. The model consisted of a 2-km-deep seawater layer with a resistivity of $0.33 \Omega \cdot \text{m}$ and anisotropic layered sea-bottom sediments (background model). A $4 \text{ km} \times 4 \text{ km} \times 50 \text{ m}$ HC reservoir structure is located at 3.5 km depth with an isotropic resistivity of $35 \Omega \cdot \text{m}$. The receivers were located at the sea bottom and spanned from -7 to 7 km in the inline (x) direction and from -4 to 4 km in the cross-line (y) direction spaced every 250 m. The source was a 300-m horizontal dipole with a frequency of 0.2 Hz. The outlines of the reservoir and source locations are shown by solid and dash-dotted lines, respectively, in Fig. 1.

We have conducted the numerical experiments similar to those presented in [7]. Fig. 1(a) presents the original plot of the normalized data, computed as the ratio of the inline electric field responses generated by a single source for the model with the HC reservoir and the corresponding background electric fields (without the HC reservoir). Fig. 1(b) shows the normalized synthetic aperture data for a synthetic aperture source without steering. Fig. 1(d) presents the normalized data produced by our optimal synthetic aperture method. In the latter case, we used designed normalized synthetic aperture data \mathbf{P} , which were introduced as a simple boxcar function covering the area of the expected reservoir anomaly [dashed line in Fig. 1(b)] detected by a single 100-m bipole source, as shown in Fig. 1(c). Note that the area of the boxcar function is larger than the area of the expected anomaly in [7] because we assume that we do not know *a priori* the exact location and size of the reservoir. One can see that our method successfully found optimal synthetic aperture weights for this model that significantly increased the ratio of the observed and background fields. The computations are very fast. It took just a few seconds for 100 iterations of inversion for this model on a computer with a 3.2-GHz Core 2 processor and 4 GB memory available.

We have also examined the effect of the noise on the synthetic aperture data. We contaminated the synthetic observed data with random Gaussian noise, which linearly increased from 1% at zero offset up to 7% at 10 000 m offset to simulate the noise behavior typical in the field data. We show in Fig. 2 (left) the maps of the fields generated from the noisy data for different synthetic aperture sources for the deep water model with an HC reservoir. Fig. 2(a) presents the normalized synthetic aperture data computed for a synthetic aperture source without steering. Fig. 2(b) shows the same data for the best steered 2-D synthetic aperture source, developed by Knaak *et al.* [7]. Fig. 2(c) presents the same data for the optimal synthetic aperture source. One can see that applying an optimal synthetic aperture method helped to increase the anomaly due to HC reservoir significantly for noisy data.

The question may arise if the developed algorithm could generate a false anomaly in the area, where there is no HC reservoir present? In order to address this question, we consider the same deep water model as above, except that there is no reservoir in this model below the seawater layer. We also assume that the background conductivity in the new model is slightly different from the original background model, e.g., by 3%, and the synthetic observed data in a new model without an HC reservoir are contaminated with noise, as was done above. Fig. 2(d) shows the synthetic aperture data without steering normalized by new background field and noise added. Fig. 2(e) shows the same data for the best steered 2-D synthetic aperture source, developed by Knaak *et al.* [7]. Fig. 2(f) presents the same data for the optimal synthetic aperture source. One can see that in the case without an HC reservoir (see Fig. 2, right), the developed algorithm does not produce any anomaly even if the selected background model is different from the true background.

V. REDUCTION OF THE AIRWAVE EFFECT IN SHALLOW WATER USING SYNTHETIC APERTURE DATA

One of the problems of interpretation of MCSEM data in shallow water is the effect of the so-called air wave, which represents the part of an EM signal from the transmitter

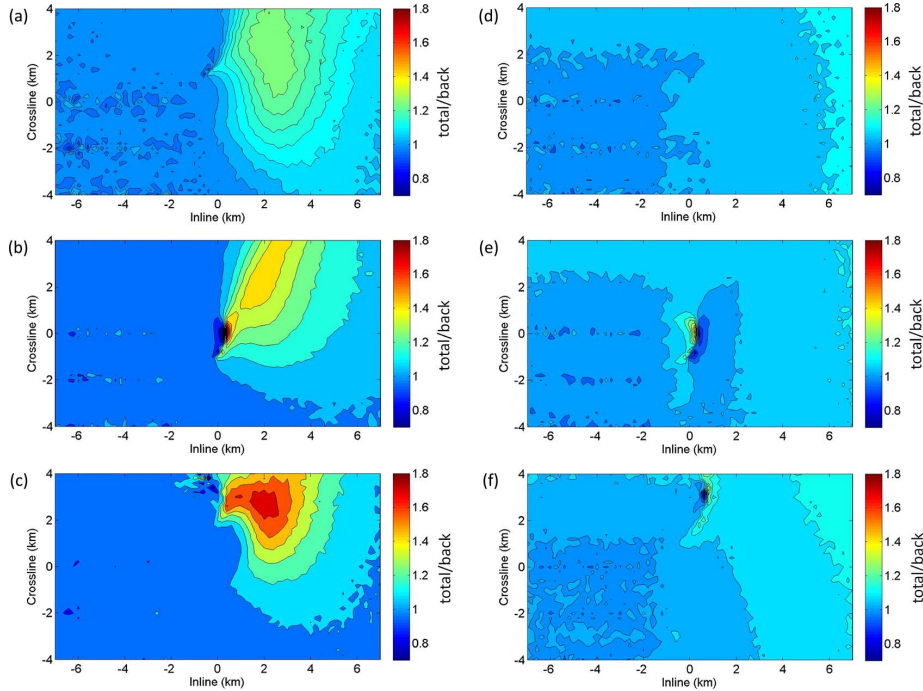


Fig. 2. Deep water model (left) with the HC reservoir and (right) without the HC reservoir. Maps of the fields generated from noisy data for different synthetic aperture sources. (a) and (d) Normalized synthetic aperture data computed for a synthetic aperture source without steering. (b) and (e) Same data for the best steered 2-D synthetic aperture source, developed by Knaak *et al.* [7]. (c) and (f) Same data for the optimal synthetic aperture source.

propagating over the sea surface. Analysis and removal of the airwave effect has been a subject of a number of publications [13], [14]. In this letter, we develop a new method of solving this problem based on the optimal synthetic aperture method.

In the original model of Knaak *et al.* [7], the authors considered deep water model (depth of the sea bottom was 2 km), in order to weaken the air wave effect at the acquisition level (sea bottom). We have designed a new model, which is similar to that of Knaak *et al.* [7] with the only difference being that in our model the water depth is just 200 m. In this case, one should expect a strong air wave effect in the observed data.

We have plotted in Fig. 3(a) the original normalized data for shallow water model, computed as the ratio of the inline electric field responses generated by synthetic aperture source for the model with the HC reservoir and corresponding background electric fields (without the HC reservoir).

Comparison of this plot with a similar plot of the data recorded in the original deep water model with the 2-km water depth [see Fig. 1(b)] shows that, in shallow water, the response from the target, i.e., the HC reservoir, is dramatically distorted by the effect of the air wave. In order to remove this distorting effect, we have designed a synthetic aperture data in a form of a boxcar function covering the area of the expected reservoir anomaly [see Fig. 3(b)]. Finally, Fig. 3(c) presents the normalized synthetic aperture data produced by our optimal synthetic aperture method based on the designed boxcar function response. We can see that the plot of the normalized synthetic aperture data in Fig. 3(c) has a regular-shaped oval structure, similar to the one shown in Fig. 1(d) for a deep-water anomaly.

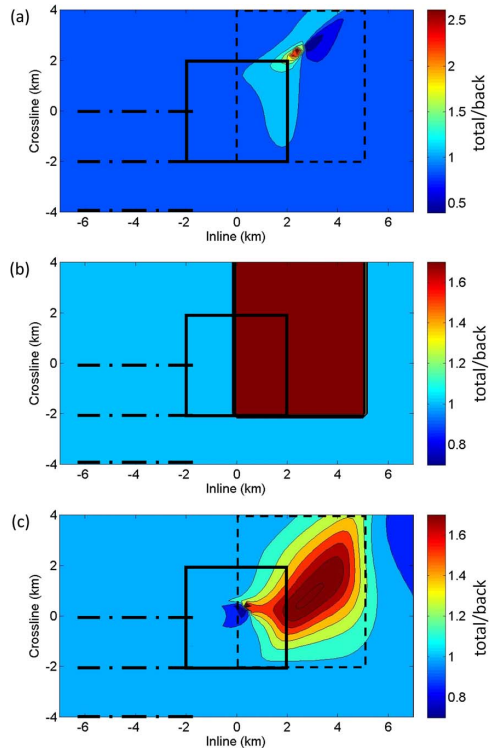


Fig. 3. Shallow water model. (a) Plot of the original normalized data. (b) Plot of the designed normalized synthetic aperture in a form of a boxcar function covering the area of the expected reservoir anomaly. (c) Normalized synthetic aperture data produced by our optimal synthetic aperture method.

VI. APPLICATION OF THE OPTIMAL SYNTHETIC APERTURE METHOD TO THE HARDING FIELD MCSEM DATA

We have applied the developed optimal synthetic aperture method to synthetic MCSEM data computer-simulated for a

Harding oil and gas field located in the U.K. sector of the North Sea, about 320 km northeast of Aberdeen.

The Harding field porosity and fluid saturation models were obtained from history-matched reservoir simulations constructed from production data, well logs, and 3-D seismic

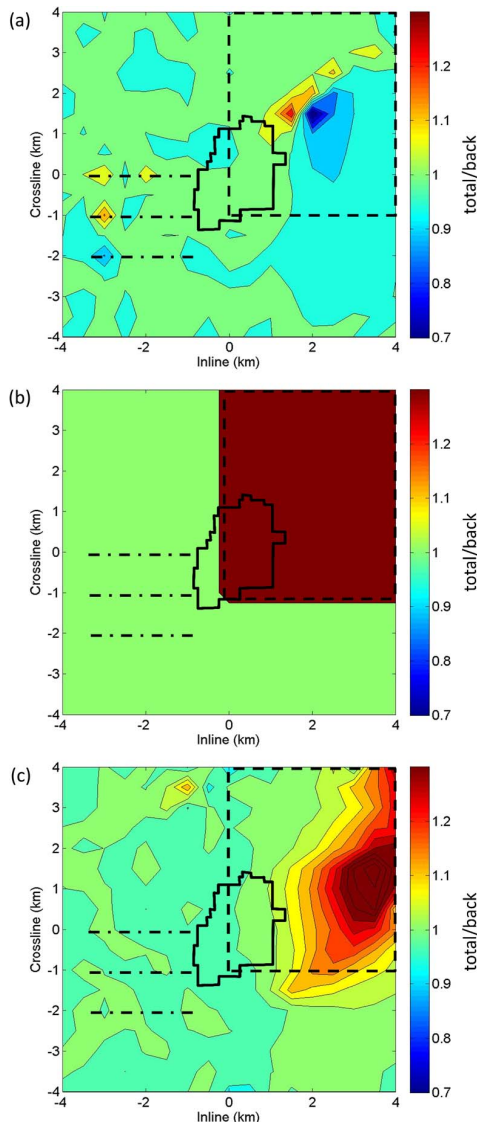


Fig. 4. Harding field model. (a) Plot of the original normalized data. (b) Plot of the designed normalized synthetic aperture in a form of a boxcar function covering the area of the expected reservoir anomaly. (c) Normalized synthetic aperture data produced by our optimal synthetic aperture method. Three MCSEM survey lines are shown by the red horizontal lines.

interpretations [15], [16]. The corresponding 3-D resistivity model consists of a 110-m $0.3\text{-}\Omega \cdot \text{m}$ water column overlying an otherwise homogeneous half-space of $1.0\ \Omega \cdot \text{m}$, in which the Harding reservoir model is embedded.

The MCSEM data were then simulated for these models and then subjected to multiple synthetic aperture scenarios. We have plotted in Fig. 4(a) the original normalized data for the Harding field model. The effect of the HC reservoir is very weak in this image due to the effect of the air wave. In order to remove this distorting effect, we used a designed synthetic aperture data in the form of a boxcar function covering the area of the expected electric field anomaly [see Fig. 4(b)]. The result of application of the optimal synthetic aperture method based on the designed boxcar function response is shown in Fig. 4(c). The electric field anomaly due to the HC reservoir clearly manifests itself in the last image.

VII. CONCLUSION

The synthetic aperture method that was introduced for the MCSEM method in [5] and [6] uses an integrated source as a combination of multiple individual sources, in order to increase the detectability of HC reservoirs. We have demonstrated in this letter that this method can be mathematically described as the data weighting with a special way of selecting the data weights in order to construct the synthetic aperture source. The main advantage of our approach is that we apply the synthetic aperture weights, variable from receiver to receiver, which is physically equivalent to “steering” the field generated from the transmitters in different directions for different receivers. As a result, we obtain better “focusing” of the transmitting EM field on the geological target, e.g., the HC reservoir. We have developed a general optimization technique to find the optimal parameters (data weights) of the synthetic aperture method. This approach makes it possible to increase the corresponding ratio between total and background fields within the area of an expected reservoir anomaly and, in this way, improve the resolution of the EM data with respect to potential subsurface targets.

REFERENCES

- [1] S. R. DeGraaf, “SAR imaging via modern 2-D spectral estimation methods,” *IEEE Trans. Image Process.*, vol. 7, no. 5, pp. 729–761, May 1998.
- [2] M. Cheney, “A mathematical tutorial on synthetic aperture radar,” *SIAM Rev.*, vol. 43, no. 2, pp. 301–312, 2001.
- [3] M. Çetin and W. C. Karl, “Feature-enhanced synthetic aperture radar image formation based on nonquadratic regularization,” *IEEE Trans. Image Process.*, vol. 10, no. 4, pp. 623–631, Apr. 2001.
- [4] A. I. Korobov, M. Y. Izosimova, and S. A. Toschov, “Development of ultrasound focusing discrete array for air-coupled ultrasound generation,” *Phys. Procedia.*, vol. 3, no. 1, pp. 201–207, Jan. 2010.
- [5] Y. Fan *et al.*, “Synthetic aperture controlled source electromagnetics,” *Geophys. Res. Lett.*, vol. 37, no. 13, pp. L13305-1–L13305-1, Jul. 2010.
- [6] Y. Fan *et al.*, “Increasing the sensitivity of controlled-source electromagnetics with synthetic aperture,” *Geophysics*, vol. 77, no. 2, pp. E135–E145, Mar. 2012.
- [7] A. Knaak, R. Snieder, Y. Fan, and D. Ramirez-Mejia, “3D synthetic aperture and steering for controlled-source electromagnetics,” *Leading Edge*, vol. 32, no. 8, pp. 972–978, Aug. 2013.
- [8] A. Kaputerko, A. Gribenko, and M. S. Zhdanov, “Sensitivity analysis of marine CSEM surveys,” in *Proc. Expanded Abstracts Soc. Exploration Geophysicists*, San Antonio, TX, USA, 2007, pp. 609–613.
- [9] D. Yoon and M. S. Zhdanov, “Controlled sensitivities for marine CSEM surveys,” in *Proc. Expanded Abstracts, Soc. Exploration Geophysicists*, San Antonio, TX, USA, 2011, pp. 599–603.
- [10] M. S. Zhdanov, “Focusing controlled sensitivity of geophysical data,” *J. Geol. Geosci.*, vol. 2, no. 1, pp. 1–5, Mar. 2013.
- [11] M. S. Zhdanov, *Geophysical Inverse Theory and Regularization Problems*. Amsterdam, The Netherlands: Elsevier, 2002.
- [12] M. S. Zhdanov and G. Keller, *The Geoelectrical Methods in Geophysical Exploration*. Amsterdam, The Netherlands: Elsevier, 1994.
- [13] L. Amundsen, L. Loseth, R. Mittet, S. Ellingsrud, and B. Ursin, “Decomposition of electromagnetic fields into upgoing and downgoing components,” *Geophysics*, vol. 71, no. 5, pp. G211–G223, Sep. 2006.
- [14] S. Constable and C. J. Weiss, “Mapping thin resistors and hydrocarbons with marine EM methods: Insights from 1D modeling,” *Geophysics*, vol. 71, no. 2, Mar./Apr. 2006.
- [15] A. Ziolkowski *et al.*, “Multi-transient electromagnetic repeatability experiment over the North Sea Harding field,” *Geophys. Prospecting*, vol. 58, no. 6, pp. 1159–1176, Nov. 2010.
- [16] M. S. Zhdanov *et al.*, “3D inversion of towed streamer EM data: A model study of the Harding field with comparison to CSEM,” *First Break*, vol. 30, no. 4, pp. 71–74, Apr. 2012.